

Two-Loop SUSY Corrections to the Anomalous Magnetic Moment of the Muon

S. HEINEMEYER^{1,2*}, D. STÖCKINGER^{3,4†} AND G. WEIGLEIN^{4‡}

¹ *CERN, TH Division, 1211 Geneva 23, Switzerland*

² *Institut für theoretische Elementarteilchenphysik, LMU München, Theresienstr. 37,
 D-80333 München, Germany*

³ *DESY Theorie, Notkestr. 85, 22603 Hamburg, Germany*

⁴ *Institute for Particle Physics Phenomenology, University of Durham,
 Durham DH1 3LE, UK*

Abstract

We calculate supersymmetric two-loop corrections to the anomalous magnetic moment of the muon, consisting of diagrams with a closed scalar fermion or fermion loop and gauge and/or Higgs boson exchange. We discuss the numerical impact of each subclass of diagrams and determine the leading contributions. We analyze in detail constraints from experimental information on the Higgs boson mass, $\Delta\rho$, and the branching ratios of $B \rightarrow X_s \gamma$ and $B_s \rightarrow \mu^+ \mu^-$. If these constraints are taken into account, the largest possible effect of our two-loop corrections is reduced from more than 3σ (in terms of the current experimental error) to $\sim 0.5\sigma$, such that the influence on the total supersymmetric prediction is smaller than previously estimated. However, exceptions arise in rather extreme parameter scenarios with a strong non-universality between the soft breaking parameters in the stop and sbottom sectors.

*email: Sven.Heinemeyer@cern.ch

†email: Dominik.Stockinger@durham.ac.uk

‡email: Georg.Weiglein@durham.ac.uk

1 Introduction

A new era of precision measurements of the anomalous magnetic moment of the muon $a_\mu \equiv (g_\mu - 2)/2$ has been initiated by the ‘‘Muon g-2 Experiment’’ (E821) at BNL, leading to the current experimental world average of [1]

$$a_\mu^{\text{exp}} = (11\,659\,208 \pm 6) \times 10^{-10} . \quad (1)$$

The most recent e^+e^- data driven evaluations of the hadronic contributions by Refs. [2–4] lead to the following Standard Model (SM) predictions (the deviation from the experimental result is also shown)¹:

$$\begin{aligned} a_\mu^{\text{theo}} &= (11\,659\,180.9 \pm 8.0) \times 10^{-10} \quad (27.1 \pm 10.0 : 2.7\sigma) [2] \\ a_\mu^{\text{theo}} &= (11\,659\,175.6 \pm 7.5) \times 10^{-10} \quad (32.4 \pm 9.6 : 3.3\sigma) [3] \\ a_\mu^{\text{theo}} &= (11\,659\,179.4 \pm 9.3) \times 10^{-10} \quad (28.6 \pm 11.1 : 2.5\sigma) [4] . \end{aligned}$$

Recent analyses concerning τ data indicate that uncertainties due to isospin breaking effects may have been underestimated earlier [4], so that with a better theoretical understanding of the isospin breaking effects the τ -based results could come closer to the e^+e^- -based results. One may thus hope that eventually a combination of e^+e^- and τ data will lead to an even more precise theoretical prediction.

While the present $\sim 2.5 - 3.3\sigma$ deviation between the SM prediction for a_μ and the experimental result can of course not be regarded as strong evidence for new physics, an increased accuracy of both theory and experiment might give rise to a significantly larger deviation in the future. On the other hand, already the current precision leads to very restrictive bounds on new physics scenarios.

This is illustrated by the fact that the experimental precision of 6×10^{-10} has now reached the level of the standard electroweak and of typical supersymmetric (SUSY) contributions. The electroweak one- and two-loop (and higher-order) contributions in the SM amount to 19.5×10^{-10} and -4.1×10^{-10} , respectively, see Refs. [5,6] for reviews. The SUSY contributions are generally suppressed by M_W^2/\tilde{M}^2 , where M_W is the mass of the W boson and \tilde{M} is the typical scale of the SUSY particle masses. However, for large values of $\tan\beta$, the ratio of the vacuum expectation values of the two Higgs doublets in the Minimal Supersymmetric Standard Model (MSSM), the muon Yukawa coupling is enhanced by $\tan\beta$ as compared to the SM. The supersymmetric one-loop contribution is approximately given by [7]

$$|a_\mu^{\text{SUSY}}| = 13 \times 10^{-10} \left(\frac{100 \text{ GeV}}{\tilde{M}} \right)^2 \tan\beta, \quad (2)$$

where all SUSY masses are assumed to be equal to \tilde{M} . The involved SUSY particles are neutralinos, charginos and scalar leptons of the second generation. The magnitude of the supersymmetric one-loop contribution is at the right level to account for the $\sim 3\sigma$ deviation between the SM prediction and the data, and even larger shifts are possible. The supersymmetric two-loop contributions are known only in some approximations. Since the one-loop

¹The numbers for the combination of the experimental and the theory error and the corresponding deviation in terms of σ have been recalculated according to the new experimental result.

contribution can be large, the two-loop corrections can be expected to be quite important, even beyond the leading QED-logarithms [8].

The importance of the SUSY two-loop contributions is twofold. On the one hand, their inclusion increases the accuracy of the bounds on the supersymmetric parameter space (see e.g. Refs. [9, 10]). On the other hand, the supersymmetric two-loop contributions depend on many additional parameters and can in principle be large even if the one-loop diagrams are suppressed due to heavy smuons and sneutrinos.

Particularly interesting contributions are the ones enhanced by large values of the Higgs mixing parameter μ and a large trilinear coupling A (where A generically denotes the Higgs–stop or Higgs–sbottom coupling, $A_{t,b}$). They arise from so-called Barr-Zee two-loop diagrams where a Higgs boson is exchanged between the external muon and a 3rd generation sfermion loop. Results for such contributions were obtained in Refs. [11, 12] and found to give huge contributions up to $\mathcal{O}(20 \times 10^{-10})$ if $\tan \beta$ is large and μ, A are of the order of several TeV. In these analyses, however, other experimental constraints on the parameter space of the MSSM were neglected. Moreover, the results of Refs. [11, 12] for the H^\pm contribution disagree by a factor 4, so that an independent check seems to be necessary.

In this paper we present a calculation and numerical analysis of all two-loop contributions Δa_μ^{2L} in the MSSM where a closed 3rd generation sfermion or fermion loop is inserted into a one-loop diagram with gauge-boson and/or Higgs-boson exchange. This set of diagrams contains the terms $\propto \mu, A$ but also other terms enhanced by the large Yukawa couplings of the t , and (for large $\tan \beta$) b, τ , as well as terms without any enhancement. All of these contributions are included in our final result.

Our numerical analysis is focused on two questions: what are the numerical results for the individual subclasses, and which of them should be taken into account for a reliable supersymmetric prediction for a_μ ? Secondly, are huge two-loop contributions of $\mathcal{O}(20 \times 10^{-10})$ still possible if existing experimental constraints on the supersymmetric parameter space are taken into account?

The rest of the paper is organized as follows. In Sect. 2 we present the two-loop diagrams and the method of their evaluation. The numerical analysis is given in Sects. 3, 4, 5. The importance of this class of two-loop corrections and their numerical size is discussed in Sect. 3, taking into account constraints on the SUSY parameter space from other experimental information. The leading contributions and the influence of the individual experimental constraints are examined in Sect. 4. Effects from non-universality of the soft SUSY-breaking parameters are analyzed in Sect. 5. We conclude with Sect. 6.

2 Calculation

In this section we briefly describe the diagrams we have investigated, their evaluation and the tools that have been used.

The set of diagrams calculated in this paper corresponds to the fermion/sfermion corrections to non-supersymmetric, i.e. two Higgs doublet model type, contributions. It forms a gauge-independent class of diagrams. In order to discuss the shift between the MSSM and

the SM predictions, we subtract the pure SM contribution from our result (where the SM Higgs boson mass M_H^{SM} is set to the value of the lightest MSSM Higgs boson mass, M_h).

The one-loop diagrams corresponding to the contributions considered in this paper are the SM one-loop diagrams. Expressing the one-loop result in terms of the Fermi constant G_μ and $s_W^2 \equiv 1 - M_Z^2/M_W^2$, (M_Z being the Z boson mass), it takes the conventional form of the electroweak one-loop result in the SM (omitting the QED contribution) [5,6],

$$a_\mu^{\text{EW,1L}} = \frac{G_\mu}{8\pi^2\sqrt{2}} m_\mu^2 \left[\frac{5}{3} + \frac{1}{3}(1 - 4s_W^2)^2 \right]. \quad (3)$$

The two-loop diagrams that we calculate can be subdivided into three classes:

($\tilde{f}V\phi$) diagrams with a sfermion ($\tilde{t}, \tilde{b}, \tilde{\tau}, \tilde{\nu}_\tau$) loop, where at least one gauge and one Higgs boson are exchanged, see Fig. 1;

($\tilde{f}VV$) diagrams with a sfermion loop, where only gauge bosons appear in the second loop, see Fig. 2;

($fV\phi$) diagrams with a fermion (t, b, τ, ν_τ) loop, where at least one gauge and one Higgs boson are present in the other loop, see Fig. 3. The corresponding diagrams with only gauge bosons are identical to the SM diagrams and give no genuine SUSY contribution.

For our later analysis we further split up the ($\tilde{f}V\phi$) diagrams of Fig. 1 into the following groups: diagrams with photon and Higgs exchange ($f\gamma\{h, H\}$), Z /Higgs exchange ($\tilde{f}Z\{h, H\}$), and W /charged Higgs exchange ($\tilde{f}W^\pm H^\mp$). The remaining sfermion loop diagrams containing only gauge boson and Goldstone boson exchange are grouped together with the diagrams involving only gauge bosons, ($\tilde{f}W^\pm G^\mp$)+($\tilde{f}VV$). All these groups are separately gauge independent in R_ξ -gauges at the order m_μ^2/M_W^2 . Note that since we neglect \mathcal{CP} -violating phases, diagrams with photon or Z and \mathcal{CP} -odd Higgs bosons A^0, G^0 do not contribute. The diagrams ($\tilde{f}\gamma\{h, H\}$) and ($\tilde{f}W^\pm H^\mp$) are the ones evaluated in Refs. [11,12] neglecting all but the leading terms in the sfermion–Higgs couplings.

All diagrams are understood to include the corresponding subloop renormalization. For the fermion loop class ($fV\phi$) we actually calculate the difference between the Standard Model and the MSSM, which originates from the extended Higgs sector of the MSSM. Diagrams where two Higgs bosons couple to the external muon are suppressed by an extra factor of m_μ^2/M_W^2 and hence negligible.

In order to perform a systematic calculation, a *Mathematica* program has been written that can deal with all kinds of MSSM two-loop contributions to a_μ . Its main steps are the following: The amplitudes for a_μ are generated using the program *FeynArts* [13,14], and the appropriate projector [15,16] is applied. The Dirac algebra and the conversion to a linear combination of two-loop integrals is performed using *TwoCalc* [17]. In order to simplify the integrals, a large mass expansion [18] is applied where the muon mass is taken as small and all other masses as large. All resulting two-loop integrals are either two-loop vacuum integrals or products of one-loop integrals. They can be reduced to the standard integrals T_{134} [19] and A_0 and B_0 [20] and can be evaluated analytically. The asymptotic expansion has to be performed up to terms of order m_μ^2 . Terms of lower power in m_μ/M_{heavy} (where M_{heavy} represents all kinds of other masses) cancel each other as required for non-QED corrections. Terms of higher powers in m_μ/M_{heavy} are numerically irrelevant and can be safely neglected.

The counterterm diagrams contain the renormalization constants $\delta M_{W,Z}^2, \delta Z_e, \delta t_{h,H}$ cor-

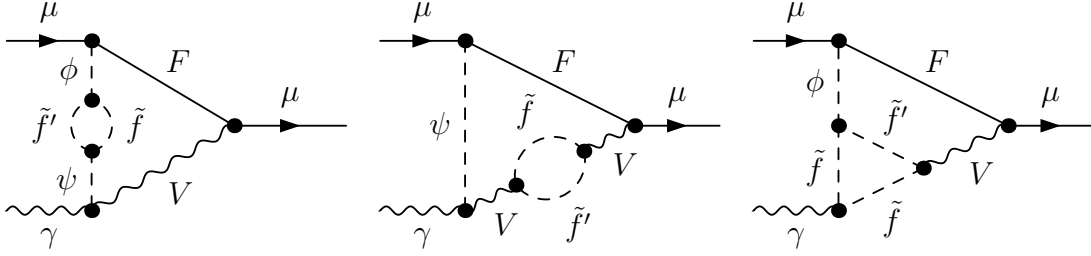


Figure 1: Some generic two-loop SUSY diagrams of type $(\tilde{f}V\phi)$ involving (at least) one gauge and one Higgs boson and a closed scalar fermion loop. $F = \mu, \bar{\nu}_\mu$; $\phi = h, H, A, H^\pm, G, G^\pm$; $\psi = G^\pm$; $f, \tilde{f} = \tilde{t}, \tilde{b}, \tilde{\tau}, \tilde{\nu}_\tau$; $V = \gamma, Z, W$. Further diagrams of this type are obtained by contracting the ψ line in the first diagram or by interchanging Higgs and vector bosons.

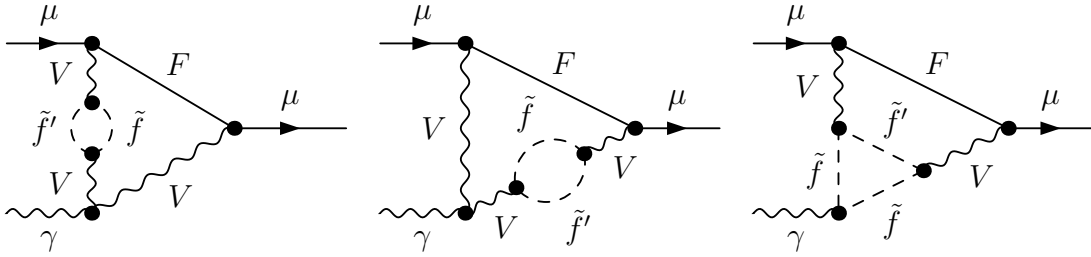


Figure 2: Some generic two-loop SUSY diagrams of type $(\tilde{f}VV)$ involving gauge bosons and a closed scalar fermion loop. $F = \mu, \bar{\nu}_\mu$; $f, \tilde{f} = \tilde{t}, \tilde{b}, \tilde{\tau}, \tilde{\nu}_\tau$; $V = \gamma, Z, W$. Further diagrams of this type involving four-point vertices exist as well.

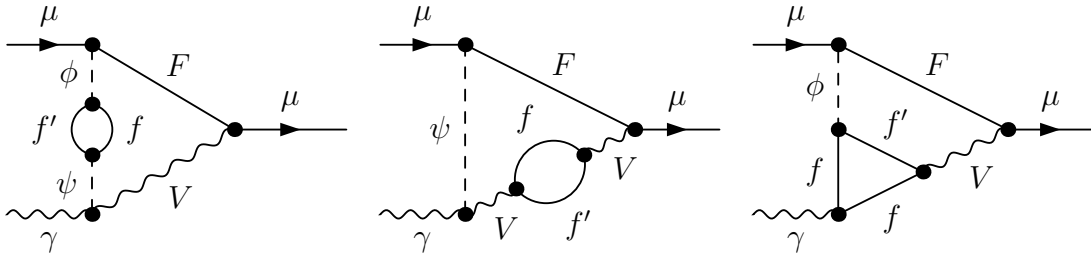


Figure 3: Generic two-loop SUSY diagrams of type $(fV\phi)$ involving (at least) one gauge and one Higgs boson and a closed SM fermion loop. $F = \mu, \bar{\nu}_\mu$; $\phi = h, H, A, H^\pm, G, G^\pm$; $\psi = G^\pm$; $f, f' = t, b, \tau, \nu_\tau$; $V = \gamma, Z, W$.

responding to mass, charge and tadpole renormalization and can be easily evaluated. We choose the on-shell renormalization scheme [21]. This leads to $\delta M_{W,Z}^2 = \text{Re}\Sigma_{W,Z}^T(M_{W,Z}^2)$, where $\Sigma_{W,Z}^T$ denote the transverse parts of the gauge-boson self-energies. The charge renormalization is given by $\delta Z_e = -1/2 \Sigma'_\gamma(0)$, where Σ' denotes the derivative of the self-energy with respect to the momentum squared. The tadpoles are renormalized such that the sum of the tadpole contribution T and the counterterm vanishes, i.e. $\delta t_{h,H} = -T_{h,H}$.

As mentioned above, see eq. (3), we are using a one-loop result which is parametrized in terms of G_μ instead of the ratio α/M_W^2 . Therefore our two-loop correction contains a term given by the product of the corresponding one-loop result and Δr , where the latter denote the one-loop corrections to muon decay, $\mu \rightarrow \nu_\mu e \bar{\nu}_e$. Relevant here are only the contributions arising from 3rd family sfermion loops to Δr . These corrections are included in our two-loop result (in the $(\tilde{f}VV)$ class).

As a cross check we have evaluated the SM two-loop diagrams with a closed fermion loop as presented in Refs. [15, 16] and found perfect agreement separately for each diagram (after going to the limit $s_W^2 \rightarrow 1/4$, used in Refs. [15, 16]). We have furthermore checked the UV-finiteness of our result as well as the cancellation of the wave function renormalization constants. We also found agreement with Ref. [12] for the contributions to the $(\tilde{f}\gamma\{h, H\})$ and $(\tilde{f}W^\pm H^\mp)$ diagrams calculated there. This confirms that the earlier result of Ref. [11] is too large by a factor of 4.

Our final result for the sum of all diagrams is rather lengthy and not displayed here. It is included as a Fortran subroutine in the code *FeynHiggs* [22] (see: www.feynhiggs.de). It can also be obtained as a *Mathematica* formula from the authors upon request.

3 Numerical results allowed by experimental constraints for the different sets of diagrams

The MSSM two-loop contributions to a_μ depend on many parameters, most notably on $\tan\beta$, the μ parameter, the trilinear soft SUSY-breaking parameters $A_{t,b,\tau}$, the mass of the \mathcal{CP} -odd Higgs M_A , and the soft SUSY-breaking parameters $M_{Q,L,U,D,E}$ appearing in the sfermion mass matrices. In Refs. [11, 12] it was shown that in particular large μ and A parameters can give rise to very large contributions of the $(\tilde{f}\gamma\{H, h\})$ and $(\tilde{f}W^\pm H^\mp)$ diagrams, however ignoring existing experimental constraints on the MSSM parameter space. In order to find out the largest possible contributions of each class of diagrams, we perform a scan of the MSSM parameter space. We vary the parameters in the ranges

$$\begin{aligned}
-3 \text{ TeV} &\leq \mu \leq 3 \text{ TeV} \\
-3 \text{ TeV} &\leq A_{t,b} \leq 3 \text{ TeV} \\
150 \text{ GeV} &\leq M_A \leq 1 \text{ TeV} \\
0 &\leq M_{\text{SUSY}} \leq 1 \text{ TeV}
\end{aligned}
\tag{4}$$

where we have set $M_{\text{SUSY}} = M_Q = M_L = M_U = M_D = M_E$ (M_Q, M_U are the soft SUSY-breaking parameters in the \tilde{t} mass matrix, M_Q, M_D in the \tilde{b} mass matrix, and M_L, M_E in the $\tilde{\tau}$ mass matrix) and $A_\tau = A_b$. Furthermore we fix $\tan\beta$ to $\tan\beta = 50$. Large values

Quantity	M_h	$\Delta\rho^{\text{SUSY}}$	$\text{BR}(B_s \rightarrow \mu^+\mu^-)$	$\Delta_{B \rightarrow X_s \gamma}$
strong bound	$> 111.4 \text{ GeV}$	$< 3 \times 10^{-10}$	$< 0.97 \times 10^{-6}$	$< 1.0 \times 10^{-4}$
weak bound	$> 106.4 \text{ GeV}$	$< 4 \times 10^{-10}$	$< 1.2 \times 10^{-6}$	$< 1.5 \times 10^{-4}$

Table 1: Strong and weak bounds imposed on the MSSM parameter space. $\Delta_{B \rightarrow X_s \gamma} = |\text{BR}(B \rightarrow X_s \gamma) - 3.34 \times 10^{-4}|$, where 3.34×10^{-4} is the current experimental central value [32].

of $\tan\beta$ and small values of M_A generically lead to larger SUSY contributions but also to more restrictive experimental constraints. These two effects tend to cancel each other. We have checked that the maximum contributions from our diagrams to a_μ allowed by the experimental constraints are about the same for $\tan\beta = 25$, $\tan\beta = 37$ and $\tan\beta = 50$ and when M_A is varied in the range $M_A = 90 \dots 150 \text{ GeV}$. The effect of relaxing the restriction of a common soft SUSY-breaking parameter in the sfermion mass matrices will be described in Sect. 5. As SM input parameters we use $m_t = 175 \text{ GeV}$, and $m_b(m_t) = 3 \text{ GeV}$ (in order to absorb leading QCD corrections).

We restrict the parameter space further by imposing the following experimental constraints:²

- The lightest \mathcal{CP} -even MSSM Higgs-boson mass M_h has to be larger than its experimental limit 114.4 GeV [25, 26].³ M_h has been evaluated with *FeynHiggs2.0* [22], based on Refs. [27–29].
- The \tilde{t}/\tilde{b} -contribution to the ρ parameter, evaluated up to the two-loop level [30], does not exceed its experimental bound.
- The branching ratios $\text{BR}(B_s \rightarrow \mu^+\mu^-)$ [31] and $\text{BR}(B \rightarrow X_s \gamma)$ [32] are in agreement with their experimental limits.⁴

In order to be able to check the sensitivity on these bounds we use a stronger and a weaker version for each bound, see Tab. 1. The two Higgs mass bounds take into account a 3 GeV uncertainty due to unknown higher-order corrections [29], the weak bound in addition an uncertainty of 5 GeV due to the imperfect knowledge of the top mass [33], on which M_h is much more sensitive than a_μ . The two bounds on $\Delta\rho^{\text{SUSY}}$, $\text{BR}(B \rightarrow X_s \gamma)$, and $\text{BR}(B_s \rightarrow \mu^+\mu^-)$ correspond to 2σ and 3σ bounds and to 90% and 95% C.L. bounds, respectively.

The interplay of these constraints restricts the allowed parameter space severely. The M_h bound puts a limit of about $2.5M_{\text{SUSY}}$ on $|A_t|$. The data on b decays constrain μ and A parameters in particular for small M_A . $\Delta\rho$ restricts the mass splittings in the \tilde{t}, \tilde{b} sectors

²There are of course also lower bounds on sfermion masses from direct searches. The bounds from LEP are roughly $m_{\tilde{t}, \tilde{b}} \gtrsim 100 \text{ GeV}$. From Run I of the Tevatron stronger bounds arise for parts of the MSSM parameter space [23, 24]. We do not impose the direct bounds explicitly in the scans since we present the results of a_μ as functions of the lightest sfermion mass.

³The limit on the SM Higgs mass holds unchanged for the light MSSM Higgs mass M_h for $M_A \gtrsim 150 \text{ GeV}$. For lower values of M_A , the bound on M_h is smaller but the restrictions implied on the μ and A parameters are significant also in this case.

⁴We are grateful to A. Dedes and G. Hiller for providing the respective codes.

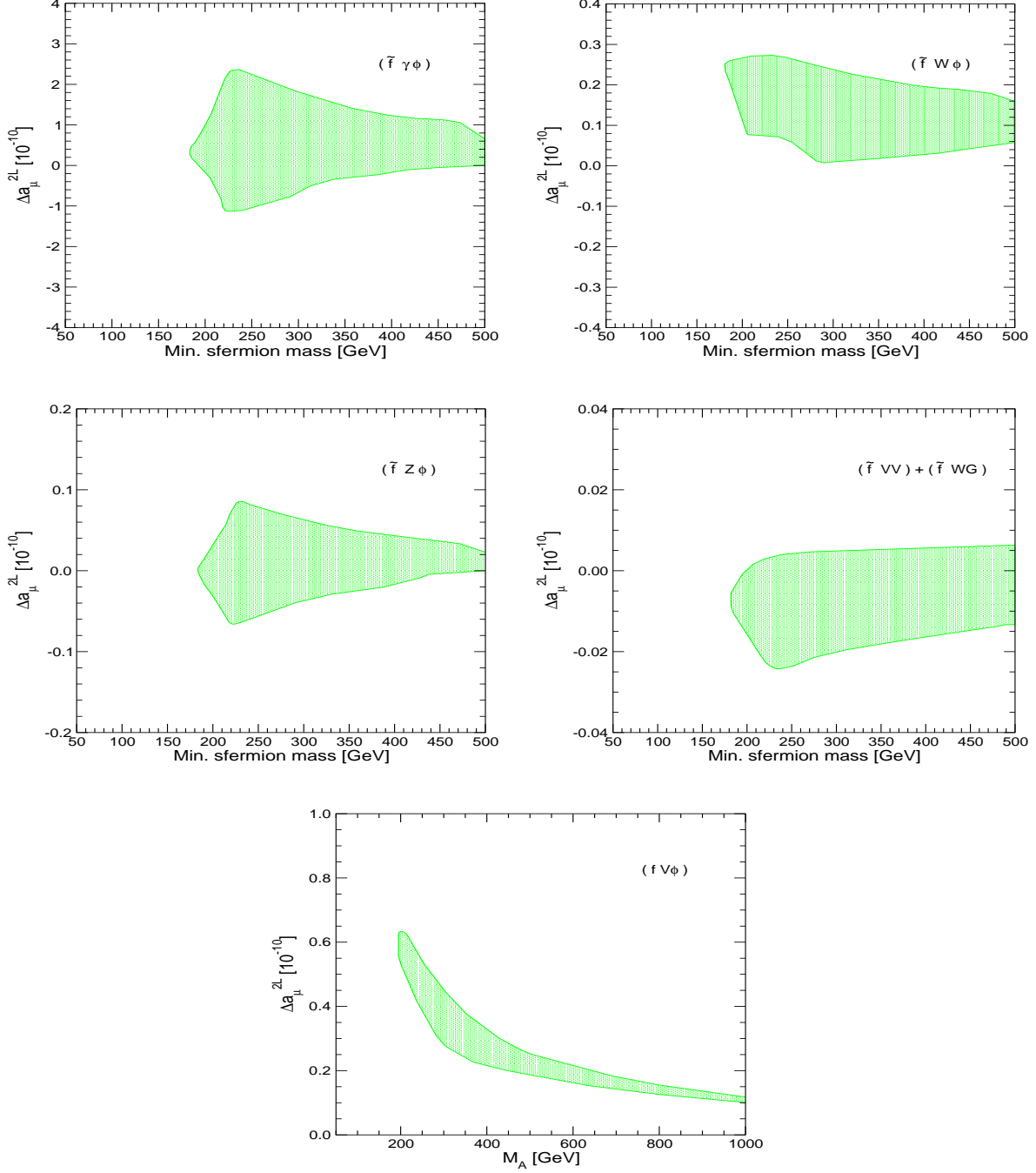


Figure 4: Possible contributions to Δa_μ^{2L} for the case that all experimental bounds are required in their strong versions. The results are subdivided into five classes of diagrams: sfermion loops with gauge and Higgs boson exchange ($\tilde{f}\gamma\{h, H\}$), ($\tilde{f}W^\pm H^\mp$), ($\tilde{f}Z\{h, H\}$), sfermion loops with gauge or Goldstone boson exchange ($\tilde{f}VV$)+($\tilde{f}W^\pm G^\mp$), and fermion loop diagrams ($fV\phi$). The results are plotted as functions of the lightest sfermion mass (sfermion loops) or M_A (fermion loops).

and thereby also the μ and A parameters, which appear in the off-diagonal elements of the squark mass matrices.

In Fig. 4 we plot the resulting ranges of possible contributions of the individual classes of diagrams for the case that all bounds are required in their strong versions. In the case of the sfermion loop contributions we plot the results for a_μ over the lightest sfermion mass ($\min\{m_{\tilde{t}_1}, m_{\tilde{t}_2}, m_{\tilde{b}_1}, m_{\tilde{b}_2}\}$), and in the case of the fermion loop contributions we plot the results over M_A .

From Fig. 4 the following conclusions can be drawn:

- The contribution of the gauge and charged Goldstone boson exchange diagrams, $(\tilde{f}W^\pm G^\mp) + (\tilde{f}VV)$, is very small. Its maximum size is about $\frac{\alpha}{2\pi}a_\mu^{\text{EW,1L}} \approx 0.02 \times 10^{-10}$.
- The contribution of the $(\tilde{f}Z\{h, H\})$ diagrams with Z and Higgs exchange is at most of the order 0.1×10^{-10} and thus negligible compared to the present experimental error. The reason for this suppression compared to the photon and W exchange diagrams is the factor $(1 - 4s_W^2)$ in the coupling of the Z to muons.
- The contribution of the $(fV\phi)$ diagrams with a fermion loop can reach 0.6×10^{-10} for small $M_A \lesssim 200$ GeV; the fermion loop diagrams are thus not completely negligible.
- The photon exchange diagrams with a sfermion loop $(\tilde{f}\gamma\phi)$ are dominant; the results of the W exchange diagrams $(\tilde{f}W^\pm H^\mp)$ are much smaller. The photon exchange diagrams are the only ones that can contribute more than 1×10^{-10} , the W exchange diagrams contribute up to 0.3×10^{-10} . The reason for the suppression of the W diagrams is not only the high value of M_W but also the fact that the W couples to two different sfermions, to $\tilde{t} - \tilde{b}$ or to $\tilde{\tau} - \tilde{\nu}_\tau$, of which at least one is usually relatively heavy.

Hence we find that the photon exchange contributions calculated in Refs. [12] are indeed the dominant subclass of diagrams with a closed (s)fermion loop. We also find, however, that the maximum contributions of more than 20×10^{-10} quoted in Refs. [11, 12] for the photon and W contributions are reduced to about 2.5×10^{-10} and 0.3×10^{-10} due to the experimental constraints on the MSSM parameter space. Owing to the smallness of these contributions, the fermion loop contributions can make up for a non-negligible part of the two-loop corrections.

4 Leading contributions and influence of the experimental constraints

Let us now focus on the photon and W exchange contributions $(\tilde{f}\gamma\{h, H\})$, $(\tilde{f}W^\pm H^\mp)$ and study the influence of the individual constraints on the ranges of possible numerical values. We choose this set of contributions not only because the photon contributions are dominant within our class of diagrams, but also because these contributions are obviously significantly restricted by the experimental constraints. In contrast, the fermion loop contributions $(fV\phi)$ can be non-negligible but depend mainly on M_A and are hardly constrained.

It is instructive to explicitly discuss the complete expression for the photon diagrams (see e.g. Ref. [12]):

$$\Delta a_\mu^{(\tilde{f}\gamma\phi),2L} = -\frac{\alpha}{\pi} \frac{G_\mu m_\mu^2}{8\sqrt{2}\pi^2} \frac{(N_c Q^2)_{\tilde{f}} \lambda_{\mu\phi} \lambda_{\tilde{f}\phi}}{M_\phi^2} \mathcal{F} \left(\frac{m_{\tilde{f}}^2}{M_\phi^2} \right), \quad (5)$$

where \tilde{f} can be one of $\tilde{t}_{1,2}$, $\tilde{b}_{1,2}$, $\tilde{\tau}_{1,2}$, and ϕ can be one of the \mathcal{CP} -even Higgs bosons, h or H . The couplings λ are defined as ($s_\alpha = \sin \alpha$, $c_\alpha = \cos \alpha$, etc.)

$$\lambda_{\mu\{h,H\}} = \{-s_\alpha, c_\alpha\}/c_\beta \quad (6)$$

$$\begin{aligned} \lambda_{\tilde{t}_i\{h,H\}} &= 2m_{t_i} \left(\mu\{s_\alpha, -c_\alpha\} + A_t\{c_\alpha, s_\alpha\} \right) U_{i1}^{\tilde{t}} U_{i2}^{\tilde{t}} / s_\beta \\ &+ \frac{6c_W m_{t_i}^2 \{c_\alpha, s_\alpha\} + M_W M_Z s_\beta (3 - 4s_W^2) \{-s_{\alpha+\beta}, c_{\alpha+\beta}\}}{3c_W s_\beta} (U_{i1}^{\tilde{t}})^2 \\ &+ \frac{6c_W m_{t_i}^2 \{c_\alpha, s_\alpha\} + 4\{-s_{\alpha+\beta}, c_{\alpha+\beta}\} M_W M_Z s_\beta s_W^2}{3c_W s_\beta} (U_{i2}^{\tilde{t}})^2 \end{aligned} \quad (7)$$

$$\begin{aligned} \lambda_{\tilde{b}_i\{h,H\}} &= 2m_{b_i} \left(-\mu\{c_\alpha, s_\alpha\} + A_b\{-s_\alpha, c_\alpha\} \right) U_{i1}^{\tilde{b}} U_{i2}^{\tilde{b}} / c_\beta \\ &+ \frac{6c_W m_{b_i}^2 \{-s_\alpha, c_\alpha\} + M_W M_Z c_\beta (-3 + 2s_W^2) \{-s_{\alpha+\beta}, c_{\alpha+\beta}\}}{3c_W c_\beta} (U_{i1}^{\tilde{b}})^2 \\ &+ \frac{6c_W m_{b_i}^2 \{-s_\alpha, c_\alpha\} - 2\{-s_{\alpha+\beta}, c_{\alpha+\beta}\} M_W M_Z c_\beta s_W^2}{3c_W c_\beta} (U_{i2}^{\tilde{b}})^2 \end{aligned} \quad (8)$$

and similar for $\lambda_{\tilde{\tau}\{h,H\}}$. The matrices $U^{\tilde{t},\tilde{b}}$ diagonalize the sfermion mass matrices $M_{\tilde{f}}^2$ in the form $U^{\tilde{f}} M_{\tilde{f}}^2 (U^{\tilde{f}})^\dagger = \text{diag}(m_{\tilde{f}_1}^2, m_{\tilde{f}_2}^2)$. The loop function \mathcal{F} is given by

$$\mathcal{F}(z) = \int_0^1 dx \frac{x(1-x) \log[z/(x(1-x))]}{z - x(1-x)}. \quad (9)$$

The result for the W contribution has a similar form.

This type of contributions can be particularly enhanced by the ratio of the mass scale of the dimensionful Higgs–Sfermion coupling divided by the mass scale of the particles running in the loop, i.e. by ratios of the form $\{\mu, A, \frac{m_{t_i}^2}{M_W}\}/\{m_{\tilde{f}}, M_{h,H}\}$, which can be much larger than one. For large $\tan \beta$ and large sfermion mixing, the leading terms are typically given by the parts of the couplings with the highest power of $\tan \beta$ and by the loop with the lightest sfermion. These contributions involve only H -exchange, since the h -couplings approach the SM-Higgs coupling for not too small M_A . They can be very well approximated by the formulas

$$\Delta a_\mu^{\tilde{t},2L} = -0.013 \times 10^{-10} \frac{m_t \mu \tan \beta}{m_{\tilde{t}} M_H} \text{sign}(A_t), \quad (10)$$

$$\Delta a_\mu^{\tilde{b},2L} = -0.0032 \times 10^{-10} \frac{m_b A_b \tan^2 \beta}{m_{\tilde{b}} M_H} \text{sign}(\mu), \quad (11)$$

where $m_{\tilde{t}}$ and $m_{\tilde{b}}$ are the masses of the lighter \tilde{t} and \tilde{b} , respectively, and M_H is the mass of the heavy \mathcal{CP} -even Higgs boson. The formulas use the approximation $\mathcal{F}(m_{\tilde{f}}^2/M_H^2)/M_H^2 \approx$

$0.34/(m_{\tilde{f}}M_H)$ for the loop function, which holds up to few percent if the respective sfermion mass fulfils $m_{\tilde{t},\tilde{b}} \lesssim M_H$. Since the heavier sfermions also contribute and tend to cancel the contributions of the lighter sfermions, these formulas do not approximate the full result very precisely, but they do provide the right sign and order of magnitude.

Equations (10), (11) show that the m_t -contributions are enhanced by one power of $\tan\beta$ from the muon Yukawa coupling and by the ratio μ/M_H , whereas the m_b -contributions contain an additional power of $\tan\beta$ from the b Yukawa coupling and the ratio A_b/M_H . For $\tan\beta = 50$ and μ and A parameters larger than 1 TeV both contributions can amount to more than 1×10^{-10} . However, μ is much more constrained by the four experimental bounds in Tab. 1 than A_b . Therefore, the largest contributions in Fig. 4 originate from the sbottom loop diagrams and from parameter constellations where \tilde{b}_1 is the lightest sfermion.

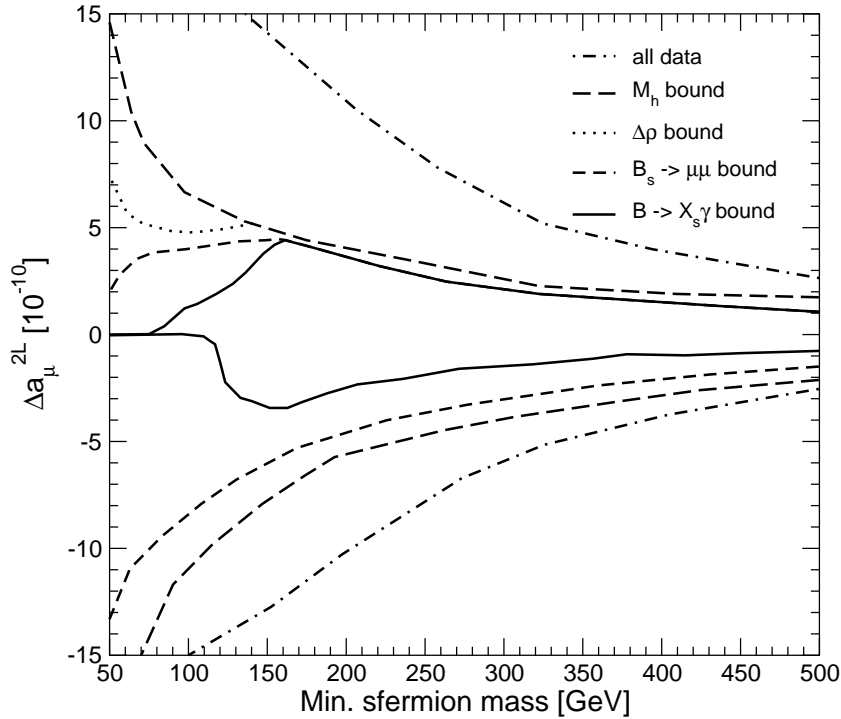


Figure 5: Maximum contributions of the $(\tilde{f}\gamma\{h, H\})$ and $(\tilde{f}W^\pm H^\mp)$ diagrams to Δa_μ^{2L} as a function of the lightest squark mass, $\min\{m_{\tilde{t}_1}, m_{\tilde{t}_2}, m_{\tilde{b}_1}, m_{\tilde{b}_2}\}$. No constraints except for the parameter ranges in eq. (4) are taken into account for the outermost curve. Going to the inner curves additional weak constraints (see text) have been applied.

Now we study the influence of the individual experimental constraints on the photon and W exchange contributions. Figure 5 is based on a data sample of ~ 300000 parameter points in the range specified in eq. (4), on which the weak versions of the bounds in Tab. 1 are incrementally applied. Figure 6 is based on the data points satisfying all weak constraints and shows the effect of strengthening each bound separately.

The results shown in Fig. 5 are the following:

- The outer lines show the largest possible results if all experimental bounds are ignored. They show a steep rise of Δa_μ^{2L} for decreasing $m_{\tilde{f}_1}$; for $m_{\tilde{f}_1} < 150$ GeV contributions

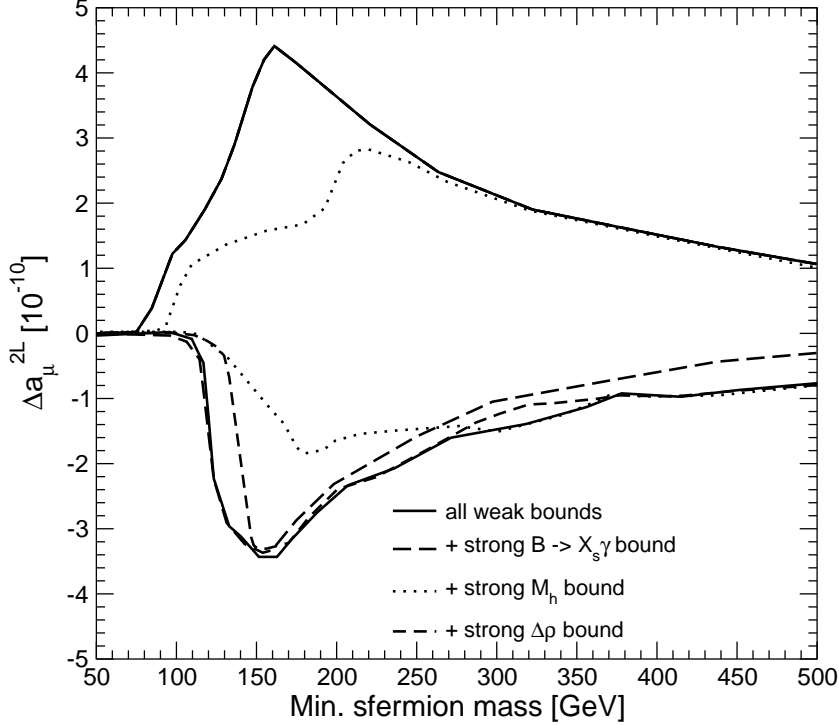


Figure 6: Maximum contributions of the $(\tilde{f}\gamma\{h, H\})$ and $(\tilde{f}W^\pm H^\mp)$ diagrams to Δa_μ^{2L} as a function of the lightest squark mass, $\min\{m_{\tilde{t}_1}, m_{\tilde{t}_2}, m_{\tilde{b}_1}, m_{\tilde{b}_2}\}$. The outer curve corresponds to weak bounds for all experimental constraints. Each inner curve takes into account one additional stronger constraint. Strengthening the $B_s \rightarrow \mu^+\mu^-$ -bound has a very small impact and is not shown. The inner area consequently corresponds to all strong constraints.

larger than 15×10^{-10} , corresponding to two standard deviations of the experimental error on a_μ , are possible.

- The next two lines show the possible results if the bound $M_h > 106.4$ GeV and then in addition the bound on $\Delta\rho$ are satisfied. The maximum contributions are very much reduced already by the M_h bound, and the $\Delta\rho$ bound reduces further the positive region for small sfermion masses. If both bounds are taken into account, $\Delta a_\mu^{2L} > 5 \times 10^{-10}$ and $\Delta a_\mu^{2L} < -10 \times 10^{-10}$ is excluded for $m_{\tilde{f}_1} \gtrsim 100$ GeV.
- The two innermost lines correspond to taking into account in addition the bound on $\text{BR}(B_s \rightarrow \mu^+\mu^-)$ and finally also on $\text{BR}(B \rightarrow X_s\gamma)$. In particular taking into account the $\text{BR}(B \rightarrow X_s\gamma)$ bound eliminates most data points with $m_{\tilde{f}_1} \lesssim 150$ GeV and thus leads to a strong reduction of the possible size of the contributions. The largest contributions of $\pm 4 \times 10^{-10}$ to Δa_μ^{2L} , corresponding to $\sim 0.7\sigma$ of the experimental error, are possible for $m_{\tilde{f}_1} \approx 150 \dots 200$ GeV.

In applying all bounds one should be aware that any flavour non-universality in the MSSM parameters could have a strong effect on the predictions for the b decays, whereas the influence on M_h and $\Delta\rho^{\text{SUSY}}$ would be mild. Hence it is interesting that even if the b physics

bounds are ignored and only the weak M_h and $\Delta\rho$ bounds are taken into account, the largest possible contributions are strongly restricted to

$$-10 \times 10^{-10} < \Delta a_\mu^{2L} < 5 \times 10^{-10} \quad (12)$$

for sfermions heavier than 100 GeV.

Figure 6 shows that strengthening the bound on M_h from $M_h > 106.4$ GeV to $M_h > 111.4$ GeV has the most significant effect. It cuts off all the regions where $\Delta a_\mu^{2L} > 3 \times 10^{-10}$ and $\Delta a_\mu^{2L} < -2 \times 10^{-10}$. Strengthening the other bounds has only a marginal effect. This confirms that the M_h -bound is most important for restricting the parameter space.

5 Non-universal soft SUSY-breaking parameters

Up to now we have found only moderate numerical effects from the two-loop diagrams with a closed (s)fermion loop, even for the photon exchange diagrams. However, the approximation formula eq. (10), $\Delta a_\mu^{i,2L} \propto \mu m_t / (m_{\tilde{t}} M_H)$, shows that values up to 15×10^{-10} should be possible if $\mu \sim 3$ TeV and $m_{\tilde{t}}, M_H \sim 150$ GeV (for $\tan\beta = 50$). In Fig. 5 such contributions indeed appear but they are excluded if the experimental constraints are taken into account. Already imposing only the bound on M_h reduces the maximum contributions almost by a factor of 3.

It is important to keep in mind that all results presented so far were based on the universality assumption $M_Q = M_U = M_D = M_L = M_E = M_{\text{SUSY}}$ for the soft SUSY-breaking parameters in the MSSM.⁵ In this section we examine the effect of relaxing this assumption. We do not attempt a full scan of the MSSM parameter space but rather investigate which pattern of non-universality can lead to particularly large results.

The reason why the large results in Fig. 5 are excluded is that universality indirectly leads to severe constraints on the μ parameter. Via universality, the left- and right-handed diagonal elements of the stop and sbottom mass matrices are linked, and if one requires a light stop, there is not much room for an even lighter sbottom. Hence the off-diagonal element in the sbottom sector cannot be much larger than the one in the stop sector, which means for large $\tan\beta$, $\tan\beta \gtrsim m_t/m_b$:

$$|\mu| \lesssim |A_t|. \quad (13)$$

A_t is not only restricted by the requirement that all stop squared masses are positive but also by the M_h -bound, which roughly leads to $|A_t| \lesssim 2.5 M_{\text{SUSY}}$. Light stops require $|m_t A_t| \approx M_{\text{SUSY}}^2$ and are therefore only possible for $M_{\text{SUSY}} \lesssim 400$ GeV, and thus $|A_t|$ can hardly exceed 1 TeV. Because of universality and eq. (13), the bounds on A_t hold also for μ , and therefore also $\mu \lesssim 1$ TeV.

⁵SU(2) gauge invariance dictates only that the same left-handed squark mass parameter M_Q appears in the stop and sbottom mass matrices (and analogously for M_L in the slepton sector). Apart from this, there is a priori no reason in the unconstrained MSSM to assume equality of the left- and right-handed sfermion mass parameters, except for simplicity. The symmetries of the MSSM allow independent values for $M_{Q,U,D,L,E}$.

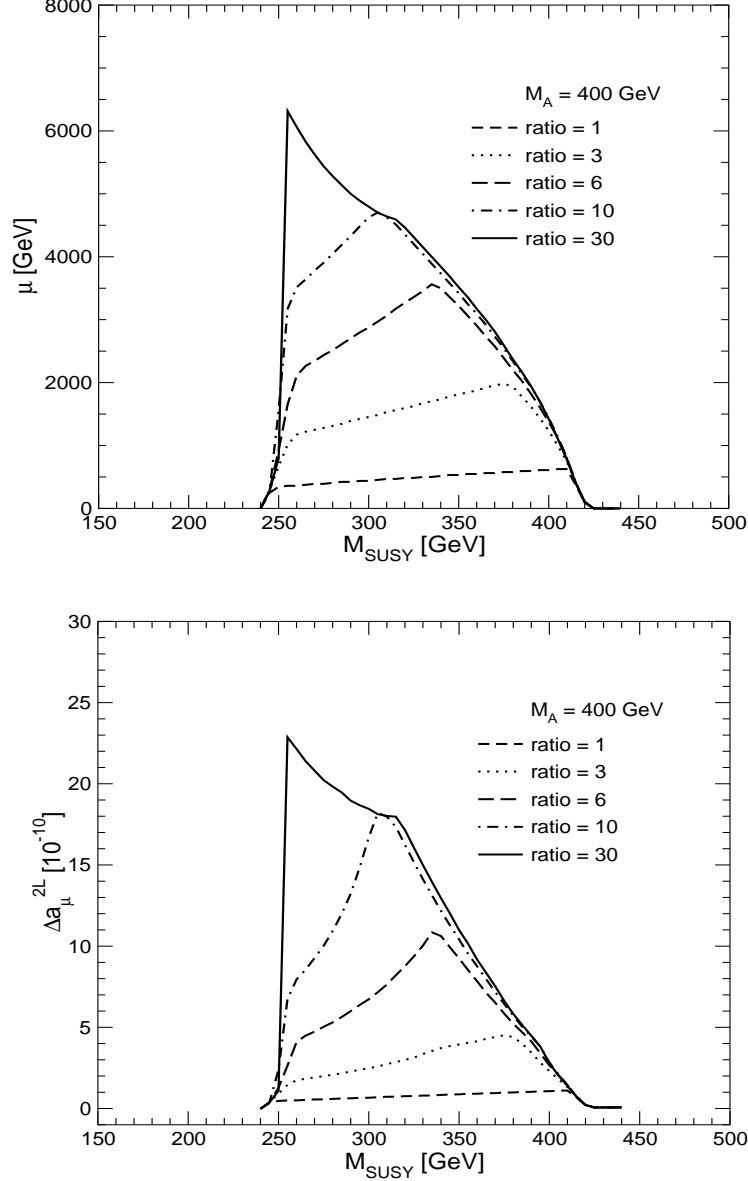


Figure 7: Possible values of μ (upper plot) and corresponding contributions to Δa_μ^{2L} (lower plot) for the case of non-universality of the soft SUSY-breaking parameters. The plots show μ and Δa_μ^{2L} as a function of $M_{\text{SUSY}} = M_Q = M_U$ for different values of the ratio M_D/M_{SUSY} . The other parameters are chosen as $m_{\tilde{t}_1} = 150$ GeV, $M_A = 400$ GeV, $A_b = 0$, $\tan \beta = 50$.

It is therefore interesting to break up the relation between the stop and sbottom mass parameters and to require only

$$M_{\text{SUSY}} = M_Q = M_U = M_L \neq M_D = M_E. \quad (14)$$

Thus we can choose small values of M_{SUSY} and A_t , giving rise to a light stop. Choosing $M_D \gg M_{\text{SUSY}}$ at the same time allows very large μ without producing a too light sbottom. We will see that these large values of μ are also compatible with the bound on M_h .

Fig. 7 shows the results for different ratios of M_D/M_{SUSY} . We choose a light stop mass

$m_{\tilde{t}_1} = 150$ GeV and a moderate value $M_A = 400$ GeV in order to avoid too strong restrictions from b decays. For each M_{SUSY} , A_t is determined by $m_{\tilde{t}_1} = 150$ GeV. The values of μ are determined as the maximum values compatible with $M_h > 111.4$ GeV and $\Delta\rho^{\text{SUSY}} < 0.004$.⁶

The upper plot in Fig. 7 shows these maximum values of μ as functions of M_{SUSY} . They significantly increase with M_D/M_{SUSY} . Already for $M_D/M_{\text{SUSY}} = 3$, values for μ larger than 1.5 TeV are possible. For $M_D/M_{\text{SUSY}} = 6$, $\mu = 3$ TeV is possible, and for $M_D/M_{\text{SUSY}} = 30$, even $\mu = 6$ TeV is possible.

The lower plot in Fig. 7 shows the corresponding results of the photon exchange diagrams $\Delta a_\mu^{(\tilde{f}\gamma\{h,H\}),2\text{L}}$. We choose $A_t < 0$ so that the contribution to a_μ is positive. The results exhibit a clear correlation with the values of μ , and they are quite precisely given by the approximation (10).⁷ Thus the maximum results with $\mu < 3$ TeV are about 10×10^{-10} , and the results for $\mu = 6$ TeV are larger than 20×10^{-10} .

It should be noted that these parameter choices are rather extreme and involve vastly different mass scales for the MSSM parameters. As an example, the largest results are obtained for $M_{\text{SUSY}} \sim 300$ GeV, $M_D \sim 9$ TeV, $A_t \sim 550$ GeV, $\mu \sim 6$ TeV. We have checked that all points plotted in Fig. 7 with $M_{\text{SUSY}} = 260 \dots 390$ GeV, where μ and $\Delta a_\mu^{2\text{L}}$ are large, satisfy not only the bounds on M_h and $\Delta\rho$ but also those on $B \rightarrow X_s\gamma$ and $B_s \rightarrow \mu^+\mu^-$. Only if smaller values, $M_A < 400$ GeV, are chosen, strong violations of the b decay bounds occur. For larger M_A , on the other hand, the b decay constraints are less restrictive, and even larger values for μ and $\Delta a_\mu^{2\text{L}}$ than in Fig. 7 are possible.

6 Conclusions

We have obtained results for MSSM two-loop corrections to the anomalous magnetic moment of the muon. The corrections consist of diagrams where a SM fermion or sfermion loop is inserted into a one-loop diagram with gauge- and/or Higgs-boson exchange. We have investigated the importance of the individual contributions and the impact of existing experimental constraints on the maximum numerical results.

It has been found that the by far most important of the considered diagrams are the ones with a sfermion loop and photon and neutral Higgs exchange ($\tilde{f}\gamma\{h,H\}$). They contribute up to about 2.5×10^{-10} in the parameter space allowed by all experimental constraints. This value has to be compared with the current experimental error of 6×10^{-10} . The diagrams with sfermion loop and W^\pm/H^\mp exchange ($\tilde{f}W^\pm H^\mp$) and the fermion loop diagrams ($fV\phi$) contribute up to 0.3×10^{-10} and 0.6×10^{-10} , respectively, while the remaining diagrams are negligible.

Our second result is that taking into account existing experimental constraints is crucial. We have carefully analyzed the impact of the constraints on the lightest Higgs-boson mass, $\Delta\rho$, $\text{BR}(B_s \rightarrow \mu^+\mu^-)$ and $\text{BR}(B \rightarrow X_s\gamma)$. If the experimental constraints were ignored and the μ and A parameters were varied up to 3 TeV, contributions of more than $15 \times$

⁶ A_b is set to zero here since the sbottom contributions cannot be expected to increase significantly beyond $\sim 5 \times 10^{-10}$, see eq. (11).

⁷Owing to the large values of μ the loop corrections to the heavy \mathcal{CP} -even Higgs mass M_H can be large, and M_H , which enters in eq. (10), can be significantly lower than M_A .

10^{-10} , corresponding to 2.5σ of the experimental error, would be possible from the two-loop diagrams. Already if only the experimental bounds on M_h and $\Delta\rho$ are taken into account, the accessible parameter space for μ , A_t , and A_b is severely restricted, and one obtains $-10 \times 10^{-10} < \Delta a_\mu^{2L} < 5 \times 10^{-10}$. Taking into account all constraints leads to the relatively small result of $\Delta a_\mu^{2L} \lesssim 3 \times 10^{-10}$. This two-loop correction of $\sim 0.5\sigma$ therefore gives rise to only a moderate shift of the one-loop SUSY result (which can easily account for the $\sim 3\sigma$ deviation between the SM prediction and the data).

The results quoted above have been obtained under the assumption of universal soft SUSY-breaking parameters $M_Q = M_U = M_D$. If one allows large mass splittings between these parameters, the considered MSSM two-loop contributions can have a significantly larger numerical effect while the existing constraints are still satisfied. We have analyzed the example of $M_D > M_Q = M_U$, which can give rise to particularly large contributions to a_μ . One needs large ratios $M_D/M_Q > 3$ and at the same time a light stop and extremely large μ in order to obtain contributions that are significantly higher than 5×10^{-10} . Though in principle possible, such parameter constellations look quite artificial, and they should be viewed as an illustration of how difficult it is to produce larger contributions to a_μ . Models with universality at some high scale typically lead to approximate low-energy universality $M_Q \approx M_U \approx M_D$ and $M_Q \gg M_L \approx M_E$, which would restrict the allowed range for μ even more than low-energy universality.

The contributions presented in this paper involve the potentially large enhancement factors $\{\mu, A\}/\{m_{\tilde{f}}, M_H\}$ and constitute an important part of the two-loop contributions in the MSSM. Our full result is included as a Fortran subroutine in the code *FeynHiggs* (see: www.feynhiggs.de). It can also be obtained as a *Mathematica* formula from the authors upon request.

In order to reduce the theoretical uncertainty of the MSSM prediction for a_μ further, the remaining two-loop contributions should be analyzed as well. The technical tools developed in this paper allow such a study, and the results will be presented in a forthcoming publication.

Acknowledgements

We thank A. Arhrib, A. Dedes, K. Desch, W. Marciano, and D. Nomura, for interesting discussions and A. Dedes and G. Hiller for providing their codes. D.S. thanks M. Steihauser and A. Freitas for useful discussions and checks of two-loop asymptotic expansion and reduction algorithms. This work has been supported by the European Community's Human Potential Programme under contract HPRN-CT-2000-00149 Physics at Colliders.

References

- [1] [The Muon g-2 Collaboration], *Phys. Rev. Lett.* **89** (2002) 101804 [Erratum-ibid. **89** (2002) 129903], hep-ex/0208001; *AIP Conf. Proc.* **675** (2003) 13, hep-ex/0301003; hep-ex/0401008.

- [2] M. Davier, S. Eidelman, A. Höcker and Z. Zhang, *Eur. Phys. J. C* **31** (2003) 503, hep-ph/0308213.
- [3] K. Hagiwara, A. Martin, D. Nomura and T. Teubner, *Phys. Lett. B* **557** (2003) 69, hep-ph/0209187;
updated by K. Hagiwara, talk given at the SUSY03, June 2003, Tucson, USA and
T. Teubner, talk given at the EPS03, July 2003, Aachen, Germany, see:
eps2003.physik.rwth-aachen.de/data/talks/parallel/11SM/11Teubner.pdf.
- [4] S. Ghozzi and F. Jegerlehner, hep-ph/0310181.
- [5] A. Czarnecki and W. Marciano, *Phys. Rev. D* **64** (2001) 013014, hep-ph/0102122.
- [6] M. Knecht, hep-ph/0307239.
- [7] T. Moroi, *Phys. Rev. D* **53** (1996) 6565 [Erratum-ibid. **D 56** (1997) 4424], hep-ph/9512396.
- [8] G. Degrossi and G. Giudice, *Phys. Rev. D* **58** (1998) 053007, hep-ph/9803384.
- [9] J. Ellis, D. Nanopoulos and K. Olive, *Phys. Lett. B* **508** (2001) 65, hep-ph/0102331;
R. Arnowitt, B. Dutta, B. Hu and Y. Santoso, *Phys. Lett. B* **505** (2001) 177, hep-ph/0102344;
J. Ellis, S. Heinemeyer, K. Olive and G. Weiglein, *Phys. Lett. B* **515** (2001) 348, hep-ph/0105061; *JHEP* **0301** (2003) 006, hep-ph/0211206;
A. Djouadi, M. Drees and J. Kneur, *JHEP* **0108** (2001) 055, hep-ph/0107316.
- [10] L. Everett, G. Kane, S. Rigolin and L. Wang, *Phys. Rev. Lett.* **86** (2001) 3484, hep-ph/0102145;
J. Feng and K. Matchev, *Phys. Rev. Lett.* **86** (2001) 3480, hep-ph/0102146;
U. Chattopadhyay and P. Nath, *Phys. Rev. Lett.* **86** (2001) 5854, hep-ph/0102157;
S. Komine, T. Moroi and M. Yamaguchi, *Phys. Lett. B* **506** (2001) 93, hep-ph/0102204;
S. Martin and J. Wells, *Phys. Rev. D* **64** (2001) 035003, hep-ph/0103067;
H. Baer, C. Balazs, J. Ferrandis and X. Tata, *Phys. Rev. D* **64** (2001) 035004, hep-ph/0103280;
S. Martin and J. Wells, *Phys. Rev. D* **67** (2003) 015002, hep-ph/0209309.
- [11] C. Chen and C. Geng, *Phys. Lett. B* **511** (2001) 77, hep-ph/0104151.
- [12] A. Arhrib and S. Baek, *Phys. Rev. D* **65** (2002) 075002, hep-ph/0104225.
- [13] J. Küblbeck, M. Böhm, and A. Denner, *Comput. Phys. Commun.* **60** (1990) 165;
T. Hahn, *Comput. Phys. Commun.* **140** (2001) 418, hep-ph/0012260.
- [14] T. Hahn and C. Schappacher, *Comput. Phys. Commun.* **143** (2002) 54, hep-ph/0105349.
- [15] A. Czarnecki, B. Krause and W. Marciano, *Phys. Rev. Lett.* **76** (1996) 3267, hep-ph/9512369; *Phys. Rev. D* **52** (1995) 2619, hep-ph/9506256.
- [16] B. Krause, PhD thesis, Universität Karlsruhe, 1997, Shaker Verlag, ISBN 3-8265-2780-1.

- [17] G. Weiglein, R. Scharf and M. Böhm, *Nucl. Phys.* **B 416** (1994) 606, hep-ph/9310358; G. Weiglein, R. Mertig, R. Scharf and M. Böhm, in *New Computing Techniques in Physics Research 2*, ed. D. Perret-Gallix (World Scientific, Singapore, 1992), p. 617.
- [18] V. Smirnov, *Applied Asymptotic Expansions in Momenta and Masses*, Springer Verlag, Berlin (2002).
- [19] A. Davydychev und J. Tausk, *Nucl. Phys.* **B 397** (1993) 123; F. Berends und J. Tausk, *Nucl. Phys.* **B 421** (1994) 456.
- [20] G. Passarino and M. Veltman, *Nucl. Phys.* **B 160** (1979) 151.
- [21] K. Aoki, Z. Hioki, M. Konuma, R. Kawabe and T. Muta, *Prog. Theor. Phys. Suppl.* **73** (1982) 1; M. Böhm, W. Hollik and H. Spiesberger, *Fortsch. Phys.* **34** (1986) 687; W. Hollik, E. Kraus, M. Roth, C. Rupp, K. Sibold and D. Stöckinger, *Nucl. Phys.* **B 639** (2002) 3, hep-ph/0204350.
- [22] S. Heinemeyer, W. Hollik and G. Weiglein, *Comp. Phys. Comm.* **124** (2000) 76, hep-ph/9812320; hep-ph/0002213; M. Frank, S. Heinemeyer, W. Hollik and G. Weiglein, hep-ph/0202166. The codes are accessible via www.feynhiggs.de .
- [23] Part. Data Group, *Phys. Rev.* **D 66** (2002) 010001.
- [24] M. Schmitt, talk given at *LeptonPhoton 2003*, Fermilab, August 2003, see: conferences.fnal.gov/lp2003/program/S2/schmitt_s02.pdf.
- [25] [LEP Higgs working group], hep-ex/0107030; LHWG Note 2001-4, see: lephiggs.web.cern.ch/LEPHIGGS/papers/ .
- [26] [LEP Higgs working group], *Phys. Lett.* **B 565** (2003) 61, hep-ex/0306033.
- [27] S. Heinemeyer, W. Hollik and G. Weiglein, *Phys. Rev.* **D 58** (1998) 091701, hep-ph/9803277; *Phys. Lett.* **B 440** (1998) 296, hep-ph/9807423.
- [28] S. Heinemeyer, W. Hollik and G. Weiglein, *Eur. Phys. Jour.* **C 9** (1999) 343, hep-ph/9812472.
- [29] G. Degrassi, S. Heinemeyer, W. Hollik, P. Slavich and G. Weiglein, *Eur. Phys. Jour.* **C 28** (2003) 133, hep-ph/0212020; A. Dedes, G. Degrassi and P. Slavich, *Nucl. Phys.* **B 672** (2003) 144 hep-ph/0305127.
- [30] A. Djouadi, P. Gambino, S. Heinemeyer, W. Hollik, C. Jünger and G. Weiglein, *Phys. Rev. Lett.* **78** (1997) 3626, hep-ph/9612363; *Phys. Rev.* **D 57** (1998) 4179, hep-ph/9710438; S. Heinemeyer and G. Weiglein, *JHEP* **0210** (2002) 072, hep-ph/0209305; hep-ph/0301062.

- [31] F. Azfar, hep-ex/0309005;
M. Nakao, talk given at *LeptonPhoton 2003*, Fermilab, August 2003, hep-ex/0312041;
K. Babu and C. Kolda, *Phys. Rev. Lett.* **84** (2000) 228, hep-ph/9909476;
S. Choudhury and N. Gaur, *Phys. Lett.* **B 451** (1999) 86, hep-ph/9810307;
C. Bobeth, T. Ewerth, F. Krüger and J. Urban, *Phys. Rev.* **D 64** (2001) 074014, hep-ph/0104284;
A. Dedes, H. Dreiner and U. Nierste, *Phys. Rev. Lett.* **87** (2001) 251804, hep-ph/0108037;
G. Isidori and A. Retico, *JHEP* **0111** (2001) 001, hep-ph/0110121;
A. Dedes and A. Pilaftsis, *Phys. Rev.* **D 67** (2003) 015012, hep-ph/0209306;
A. Buras, P. Chankowski, J. Rosiek and L. Slawianowska, *Nucl. Phys.* **B 659** (2003) 3, hep-ph/0210145;
A. Dedes, *Mod. Phys. Lett.* **A 18** (2003) 2627, hep-ph/0309233.
- [32] P. Cho, M. Misiak and D. Wyler, *Phys. Rev.* **D 54**, 3329 (1996), hep-ph/9601360;
A. Kagan and M. Neubert, *Eur. Phys. J.* **C 7** (1999) 5, hep-ph/9805303;
K. Chetyrkin, M. Misiak and M. Münz, *Phys. Lett.* **B 400**, (1997) 206, [Erratum-ibid. **B 425** (1998) 414] hep-ph/9612313;
P. Gambino and M. Misiak, *Nucl. Phys.* **B 611** (2001) 338, hep-ph/0104034;
A. Ali, E. Lunghi, C. Greub and G. Hiller, *Phys. Rev.* **D 66** (2002) 034002, hep-ph/0112300;
R. Barate et al. [ALEPH Collaboration], *Phys. Lett.* **B 429** (1998) 169;
S. Chen et al. [CLEO Collaboration], *Phys. Rev. Lett.* **87** (2001) 251807, hep-ex/0108032;
K. Abe et al. [Belle Collaboration], *Phys. Lett.* **B 511** (2001) 151, hep-ex/0103042;
B. Aubert et al. [BABAR Collaboration], hep-ex/0207074; hep-ex/0207076.
- [33] S. Heinemeyer, W. Hollik and G. Weiglein, *JHEP* **0006** (2000) 009, hep-ph/9909540.